

3043  
26 Mar 1984

## DRAG MEASUREMENTS OF LONG CABLES IN THE OCEAN

ROGER A. HOLLER  
Naval Air Development Center  
Warminster, Pennsylvania 18974

### Abstract:

Concern about the high coefficients of drag measured on short-length vibrating cables by various investigators initiated a joint NAVAIRDEVCON-MIT effort to measure coefficients of drag on long cables in the ocean environment. The experiments were conducted in December 1983 in deep waters just north of St. Croix, USVI. Top angle and tension measurements of the suspended cables were made and acceleration measurements using orthogonal pairs of accelerometers attached to the cables at various locations were recorded. The current environment was measured using current meters suspended from the test platform and expendable current profilers. Tension and inclination measurements were compared to computer simulations of the experiment to determine effective cable drag coefficients. The acceleration data were integrated to determine strumming amplitudes from which local coefficients of drag could be derived. The two methods of evaluating drag were compared and found to yield comparable results. Acceleration spectra were tested for correlation between vibration at separated locations on the cable and were generally found to be uncorrelated. The data support the argument that in realistic ocean currents, long cables exhibit lower coefficients of drag than their shorter counterparts in the uniform flow conditions of the laboratory experiments and that strumming is not correlated along the entire cable length.

PRELIMINARY

## INTRODUCTION

1. In the development of sonobuoys and oceanographic moored systems, design requirements to achieve desired performance are predicated upon how the system is characterized in analytical models simulating it in a selected environment. Of primary importance to this effort are the assumptions made for hydromechanical parameters.
2. Since a moored system has a long cable connecting the anchor and the surface float, the cable drag is a significant factor in the design of the system. The cable drag has a driving impact on cable strength, cable length, surface float design, and anchor design and, in a limited volume system, can determine whether or not the system is feasible.
3. Recent experimental data have indicated that the drag coefficient of oceanographic cables, as a result of cable strumming, can be very large, i.e., on the order of 2.5 to 3.0 instead of the 1.4 value generally used. Because the high values cited arose from experiments with short cables in modal vibration in a uniform flow field, it was considered unlikely that these values applied directly to long ocean-deployed cables that were subjected to non-uniform shear currents.
4. Because of the critical nature of the drag in moored systems, it was decided that an experiment should be undertaken in the ocean to measure the drag of long cables in realistic flow fields. The experiment was conducted in St. Croix, USVI, in late November and early December 1983, by the Naval Air Development Center and the Massachusetts Institute of Technology.

## BACKGROUND

1. The drag of a body is defined as:

$$F_D = \rho/2 C_D A V^2$$

(1)

Where  $F_D$  is the drag force,  $\rho$  is the density of the fluid,  $A$  is the area of the of the body normal to the flow,  $V$  is the velocity of the fluid past the body, and  $C_D$  is the drag coefficient. For a cylinder of large length-to-diameter ratio, representing a cable, the drag per unit length is:

$$F_{D, L} = \rho/2 C_D d V^2 \quad (2)$$

where  $d$  is the diameter of the cylinder. The drag coefficient for an infinite cylinder normal to the flow has been experimentally determined by many investigators and is shown in figure 1 as a function of the Reynolds number:

$$N_{Re} = Vd/\gamma \quad (3)$$

where  $\gamma$  is the kinematic viscosity of the fluid.

2. When a cylinder or a cable is subjected to a transverse flow, a pair of vortices form in the wake of the cylindrical body and eventually begin to shed alternately (if  $N_{Re} > 50$ ). These shedding vortices develop and shed with a frequency directly proportional to the velocity:

$$f_s = \frac{St V}{d} \quad (4)$$

where  $f_s$  is the shedding frequency and  $St$  is the nondimensional Strouhal number. This phenomenon of vortex formation is the well-known von Karman effect and the shedding frequency is often called the Strouhal frequency. The Strouhal number has been established empirically and is shown in figure 2 as a function of Reynolds number.

3. When the shedding frequency corresponds to a natural frequency mode of the elastically suspended cylinder or the flexible cylinder, the vortex shedding excites oscillation at the natural frequency. For a cable, the string equation is

$$f_n = \frac{n}{2L} \sqrt{T/m_c} \quad (5)$$

where  $f_n$  is the natural frequency of the  $n^{\text{th}}$  mode,  $L$  is the cable length,  $T$  is the tension in the cable, and  $m_c$  is the mass per unit length of the cable. The fluid excitation of a cable by von Karman vortices is called strumming.<sup>1, 2</sup>

4. Sonobuoy cable strumming has been of considerable concern to the Navy because of the mechanically coupled noise which can arise in a hydrophone suspended from a strumming cable unless the hydrophone is sufficiently isolated or the strumming impeded through the use of fairings.<sup>3</sup> It has long been recognized that strumming increases the drag of a cable and early estimates of the drag coefficient for strumming cables were made in 1967 by Dale, McCandless, and Holler<sup>4</sup> to be  $C_{DS} = 1.4$ , and this value has been used for sonobuoy systems since that time.

5. More recent measurements in the laboratory and under relatively constant flow conditions in the field have resulted in drag coefficients which are considerably higher. Vandiver and Griffin<sup>5</sup> and McGlothlin<sup>6</sup> report on some experiments in a natural flow channel above a sandbar at the mouth of Holbrook Cove, near Castine, Maine. The tidal currents provided nearly uniform flow over the 75 foot test "cable", an instrumented piece of flexible PVC tubing 1.25 inches

in diameter. Data was reported in the 0.8 to 2.4 ft/s range ( $5800 \leq N_{Re} \leq 17,000$ ) resulting in measured drag coefficients in the first six strumming modes from  $C_D = 2.4$  to 3.2.

6. If ocean systems were required to accomodate drag coefficients of the magnitude measured at Castine, a radical change in design would be dictated. On the other hand, experience with many ocean deployed sonobuoys and moored systems, both by the Navy and by others, such as the Woods Hole Oceanographic Institute, seems to contradict very high drag coefficients for cables in the ocean. Alexander<sup>7</sup> investigated long tow-wires and arrived at a drag coefficient of  $1.791 \pm 0.020$  over the Reynolds number range  $7000 \leq N_{Re} \leq 12,000$ , which is closer to values normally estimated.

### Drag Equations

1. In order to put the problem in perspective, it is instructive to consider the empirical equations used to describe the strumming cable. The local drag of a strumming flexible cylinder, or cable, is related to the near wake pattern behind it and can be described, according to Skop, Griffin, and Ramberg<sup>8</sup>, using the wake response parameter  $W_r$ ; defined by

$$W_r = [1 + 2y/d] (\omega / \omega_s) \quad (6)$$

where  $y$  is the peak amplitude at the antinode,  $d$  is the cable diameter,  $\omega$  is the angular frequency of vibration, and  $\omega_s$  is the Strouhal angular frequency:

$$\omega_s = 2\pi f_s = 2\pi \frac{StV}{d} \quad (7)$$

where  $St$  is the Strouhal number and  $V$  is the free stream velocity past the cylinder, and  $f_s$  is the Strouhal frequency.

2. When strumming is locked-on at a natural frequency of the cylinder system,

$$\omega \approx \omega_n \approx \omega_s \quad (8)$$

where  $\omega_n$  is the system natural angular frequency. Therefore, in modal strumming, the wake response parameter at the antinode is:

$$W_r = 1 + 2y/d \quad (9)$$

3. The ratio of the drag coefficient of the strumming cable at the antinode to the drag coefficient of the non-vibrating cable is

$$C_{DS}/C_{D0} = 1.0 \quad W_r < 1 \quad (10)$$

$$C_{DS}/C_{D0} = 1.0 + 1.16 [W_r - 1]^{0.65} \quad W_r \geq 1 \quad (11)$$

Substituting for  $W_r$  in the last equation:

$$C_{DS}/C_{D0} = 1.0 + 1.16 (2y/d)^{0.65} \quad (12)$$

Therefore, if the antinode amplitude is known, the drag coefficient can be calculated.

4. Griffin, Ramberg, Skop, Meggitt, and Sergev<sup>9</sup> summarize amplitudes predicted by several sources as follows:

Griffin, Skop, and Ramberg:

$$y/d = \frac{1.29 \gamma}{[1 + 0.43(2\pi St^2 ks)]^{3.35}} \quad (13)$$

Blevins:

$$y/d = \frac{0.07 \gamma}{(1.9 + ks)St^2} \left[ 0.3 + \frac{0.72}{(1.9 + ks)St} \right]^{\frac{1}{2}} \quad (14)$$

Sarpkaya:

$$y/d = \frac{0.32 \gamma}{[0.06 + (2\pi St^2 ks)^2]^{\frac{1}{2}}} \quad (15)$$

where  $\gamma = 1.16$  for a sinusoidal mode shape (cable), and  $ks$  is reduced damping.

5. Figure 3 shows  $C_{DS}/C_{D0}$  as a function of  $ks$  determined by substituting equations (13), (14), and (15) into equation (12) where  $St = 0.21$ . Large values of  $C_{DS}$  are predicted by these curves. Mc Glothlin<sup>6</sup> utilized the Skop, Griffin, and Ramberg expression (equation (12)) to find the average drag coefficient for the vibrating, flexible cylinder by replacing the local amplitude with the mode shape and integrating over the length of the cable. This resulted in the following relation based on the antinode displacement  $y$ :

$$C_{D,AVG}/C_{D0} = 1 + 0.833 \left( \frac{2y}{d} \right)^{0.65} \quad (16)$$

and equivalently, Vandiver and Griffin<sup>5</sup> express this as

$$C_{D,AVG}/C_{D0} = 1 + 1.043 \left( \frac{2 y_{rms}}{d} \right)^{0.65} \quad (17)$$

where  $y_{rms}$  is the root-mean-square of the antinode displacement. Figure 3 shows the average  $C_{D,AVG}$  for the envelope of  $y/d$  values obtained from equations (13), (14), and (15). Experimental data obtained in tests with instrumented flexible cylinders and "cables" constructed of steel tubing and PVC tubing, respectively, in low model vibration showed good agreement with equations (16) and (17).

6. In order to determine  $C_{D,AVG}/C_{D0}$  for a particular cable, the reduced damping must be evaluated. Skop, Griffin, and Ramberg determined that the reduced damping,  $ks$ , can be expressed as

$$ks = \pi c / 2 \rho \gamma \beta n \quad (18)$$

where  $\rho$  is the fluid density,  $\gamma$  is the kinematic viscosity of the fluid,  $\beta n$  is the vibratory Reynolds Number at the natural frequency:

$$\beta n = \omega_n d^2 / 4 \gamma \quad (19)$$

and  $c$  is the viscous damping per unit length at  $\omega_n$  and is dominated by the fluid contribution so that

$$c \approx 4.5\pi\gamma\beta n^{\frac{1}{2}} \quad (20)$$

Substituting for  $\beta n$ ,

$$k_s = 22.2/\beta_n^{\frac{1}{2}} \quad (21)$$

or

$$k_s = 22.2/\sqrt{\frac{\omega_n d^2}{4\gamma}} = \frac{44.4}{d} \sqrt{\frac{\gamma}{\omega_n}} \quad (22)$$

at lock-on

$$\omega_n = \omega_s = 2\pi \frac{StV}{d} \quad (23)$$

and

$$k_s = \frac{44.4}{d} \sqrt{\frac{\gamma d}{2\pi StV}} = 44.4 \sqrt{\frac{\gamma}{2\pi StVd}} \quad (24)$$

Evaluating at  $\gamma = 1.3 \times 10^{-5} \text{ ft}^2/\text{S}$  and  $St = 0.21$ ,

$$k_s = 0.139/\sqrt{Vd} \quad (25)$$

7. Equation (24) can also be written

$$k_s = 17.7/\sqrt{StN_{Re}} \quad (26)$$

and for  $St = 0.21$

$$k_s = 38.6/\sqrt{N_{Re}} \quad (27)$$

Using the Griffin, Skop, and Ramberg antinode amplitude of equation (13) and the average  $C_D$  of equation (16)

$$C_{D,AVG}/C_{D0} = 1 + 0.833 \left[ \frac{2.993}{[1 + 4.6/\sqrt{N_{Re}}]^{3.35}} \right]^{0.65} \quad (28)$$

$$C_{D,AVG}/C_{D0} = 1 + 1.699 \left[ \frac{1}{[1 + 4.6/\sqrt{N_{Re}}]} \right]^{2.1775} \quad (29)$$

For the range of  $500 \leq N_{Re} \leq 20,000$  where  $St$  can be approximated by 0.21, equation (29) is shown in Figure 4. Using values of  $C_{D0}$  from Figure 1, the curve of  $C_{D,AVG}$  vs. Reynolds number is shown in Figure 5.

## DISCUSSION

1. A test to measure coefficients of drag on long cables in the ocean was conducted jointly by the Naval Air Development Center and the Massachusetts Institute of Technology from 30 November to 3 December 1983, in the 12,000 ft. deep water six miles north of Christiansted, St. Croix, USVI. The tests were performed aboard the US Navy Barge YFN-1126, a 137 ft. long by 34 ft. wide vessel which provides a stable operating platform. The barge is self-powered and normally transits to and is tethered to a buoy permanently moored in the deep water.
2. Two current meters suspended from the barge to different depths were used in concert with Sippican XCP's (Expendable Current Profilers) to record the water velocities relative to the test cables. Three types of cables were used: a 0.16 -inch diameter kevlar cable with built-in accelerometers provided by MIT (the MIT cable), a 0.094-inch diameter kevlar cable (the RDSS cable), and a 50-ft. elastomer of 0.75-inch unstretched diameter with 232-ft. of 0.15-inch diameter electrical cable attached (the bungee).
3. Two methods were used to evaluate the drag of the cables. The first method consisted of measuring top angle and tension of the cable which was suspended from the test platform. At the bottom of the cable, a weighted, faired cylinder 12-inches high by 5-inches in diameter with an aspect ratio of 4-to-1 (see figure 6) was attached. This lower unit had been fabricated at the Naval Air Development Center and towed in the NADC Open Water Facility to measure its drag. Computer simulations of the suspended cable with the lower unit in the measured current were compared with the tilt and tension data to determine a total drag coefficient for the cable. The second method consisted of measuring accelerations of the cable at various locations using pairs of orthogonally positioned accelerometers. From these data, amplitude of vibration was calculated and local drag coefficients at the location of each pair of accelerometers determined from the equations previously developed (e.g. eq. (11) and eq. (12)) and correlation of spectra from accelerometer pairs at different locations on the same cable was tested to determine the extent to which strumming at one point on the cable was related to that at another point separated by a known distance.
4. Figure 7 shows the physical arrangement of the sensors. In addition to the two pairs of built-in accelerometers in the MIT cable, two pairs of roving biaxial accelerometers were available to attach to the cables at shallow locations. Figure 8 shows the experimental set-up of the electronics. Real time chart recordings of all tilt, tension, and current meter data were made using an 8-channel Gould strip chart recorder. All accelerometer data, in addition to the tilt, tension, and current data, were recorded on a Honeywell 101 tape recorder. Selected data were also recorded on the MIT 4-channel tape recorder to facilitate early analysis. The Naval Air Development Center was responsible for the measurement of the tilt and tension and the derivation of drag coefficients from this method, and MIT was responsible for the accelerometer measurements and the assessment of local drag coefficients and strumming correlation from this method.

### Drag Coefficients From Cable Inclination Measurements

1. Although ten different experimental cable configurations were tested, not all were useful in the drag measurements made by the tilt-tension method. On

1 December, the barge was tethered to the mooring. The ambient currents were small, mainly less than 0.3-knot, resulting in small angles of inclination of the cable as measured from the vertical. Similarly, the computer simulations of the systems subjected to these small currents yielded small angles over the range of  $C_D$  from 1.0 to 3.0. The evaluation of drag coefficients based on these small angles would be subject to large error and could be misleading. This was recognized to be a problem during the test, and it was decided that for the testing on 2 December the barge would be untethered and measurements would be made with the barge underway, heading into the wind. Experiments 3 through 6 were performed under these conditions. On 3 December, the seas were too rough to allow the barge to untether from the mooring buoy safely. It was decided to attempt to impart more relative water velocity to the system by backing the barge away from the buoy to which it was tethered, pulling slack out of the mooring cable catenary, then to let the mooring pull the barge toward it as it returned to its normal configuration. This was a viable concept; however, it was determined later that the long cables (2000 ft. to 9000 ft.) that were being tested this way were not in equilibrium during the test. The motion of the barge served to change the catenary of the test cables but did not act long enough in one direction to yield valid data.

2. Experiments 4 and 5 used 630 ft. and 950 ft. of MIT cable, respectively. The computer generated inclination angle vs. speed of tow by the barge for various coefficients of drag along with measured data for these two experiments are shown in figures 9 and 10. Although there is considerable scatter in the data, it is apparent that the drag coefficients fall in the 1.0 to 2.0 range and not in the 2.0 to 3.0 range which would be predicted on the basis of anti-nodal amplitudes of low mode vibration. The data are shown as a function of Reynolds number in Figure 11, where the mean is  $C_D = 1.41$ .

3. Experiment 3 was the bungee composite cable. On the basis of the stress-strain data taken at dockside for the bungee under test, a composite diameter of 1.1-inch over a length of 68 ft. was used to describe the cable. This was based on conservation of frontal area for the bungee as opposed to conservation of volume, which yielded a slightly larger (1.777-inch) diameter, as a conservative approach. Figure 12 shows the data for this configuration, where the Reynolds number based on the bungee (elastomer) stretched diameter of 0.59-inches is in the range 5000 to 9000, where as the Reynolds number range for the 0.15-inch diameter electrical cable is 1300 to 2300, similar to that of the MIT cable. If the drag coefficient for the overall configuration is related to drag coefficients for the two components:

$$(C_D A)_{\text{composite}} = (C_D A)_{\text{bungee}} + (C_D A)_{\text{elect. cable}} \quad (30)$$

and substituting for the calculated areas

$$6.24 C_D \text{ composite} = 3.34 C_D \text{ bungee} + 2.90 C_D \text{ elect. cable} \quad (31)$$

The  $C_D$  for the bungee can be expected to be larger than the  $C_D$  for the electrical cable because of the higher Reynolds number for the bungee, as indicated by Figure 1, 4, and 5. A reasonable agreement with the data of Figure 12 is obtained if the  $C_D$  for the electrical cable is selected to be 1.4 and the  $C_D$  for the bungee is 2.0, yielding a composite  $C_D$  of 1.73.

4. In experiments 4 and 5, the higher near surface current was considered not to affect the drag measurements because it acted over a small percentage of the



cable (~5%). In experiment 3, the bungee was suspended below a 47 ft. small diameter (0.094-inch) cable, again reducing the affect of the surface current to a negligible quantity. In experiment 6, however, an 875-ft. length of the MIT cable was suspended below the bungee-composite, which was, now, in the surface current. Using the composite  $C_D$  for the bungee of 1.73, Figure 13 shows the angle vs. speed for various drag coefficients for the MIT cable, neglecting the surface current. By superimposing various surface differentials and further assuming a  $C_D = 1.4$  for the MIT cable, it is seen from Figure 14 that a small differential current (0.3 knots) acting on the large bungee approximates the measured data.

5. On the basis of these measurements, a Reynolds number dependent  $C_D$  may be suggested, but the values are not nearly as large as predicted by Figure 5. A modification to the Griffin, Skop, and Ramberg formulation (eq. (13)) for long cables would seem to be appropriate as a tentative approach to the drag of long cables:

$$y^*/d = \frac{0.45}{[1 + 0.43(2\pi St^{2ks})]^{3.35}} \quad (32)$$

Substituting this into eq. (16) with the other assumptions of eq. (27) and  $St = 0.21$ ,

$$C_{D, AVG}/C_{D0} = 1 + 0.778 / \left(1 + \frac{4.6}{\sqrt{N_{Re}}}\right)^{2.1775} \quad (33)$$

Using this formulation and the  $C_{D0}$  values of Figure 1,  $C_{D, AVG}$  vs.  $N_{Re}$  was plotted in Figure 15. The values reflect the experimental values of this test and agree well with Alexander's<sup>7</sup> measurements. The implications of this formulation is that the average antinodal-equivalent amplitudes in long cables is 30% of the anti-node amplitudes for short cables in modal vibration. For the MIT cable in the 1200 to 2200 Reynolds number range, the antinodal-equivalent amplitudes from

$$\frac{y^*}{d} = \frac{0.45}{\left[1 + \frac{4.6}{\sqrt{N_{Re}}}\right]^{3.35}} \quad (34)$$

are  $0.33 \leq y^*/d \leq 0.43$  and the RMS amplitudes are  $0.233d \leq y^*_{rms} \leq 0.304d$ .

#### Drag Coefficients From Cable Acceleration Measurements

1. The drag from accelerometer pairs attached to the cable at various locations were recorded and analyzed by MIT. Figure 16 and 17 show typical data as collected from Experiment 1 in which 950 ft. of the MIT cable was suspended from the barge tethered to the moor. The accelerometers were 75 ft. and 350 ft. down the cable in figures 16 and 17, respectively. As can be seen from the acceleration spectra, discrete frequencies which are caused by localized strumming can be seen, but the frequencies for the two locations are different. The acceleration data is integrated twice to obtain displacement spectra which, in turn, are used to determine the RMS displacement of the cable. The values obtained in Figures 16 and 17 for RMS displacement are 0.129d and 0.126d, respectively, which when used in eq. (17) give  $C_{D, AVG}/C_{D0}$  values of 1.432 and 1.426. The Reynolds number for this experiment was around 500 where  $C_{D0} \approx 1.0$ . This  $C_{D, AVG} \approx 1.43$  was in good agreement with the results obtained from the angle measurements.

2. In general, the RMS amplitudes measured were from  $0.1d$  to  $0.4d$ , which is low compared with amplitudes predicted from low mode vibration in uniform flow, indicating that the long cable is not locked-in the way a short cable can be. This is evident, also, from the correlation analysis. There was no correlation between vibration at separate locations on the cable as close together as 100 ft. A detailed report describing the accelerometer measurements and consequent analysis and conclusions, including a model to predict the behavior of long cables in flow, will be issued by MIT.

### Factors Influencing Long Cable Vibration

1. It is not an altogether surprising result that the behavior of a long cable in variable flow is not the same as that of a short cable in uniform flow. Several factors are involved, including the flow field variation, the geometry of the cable, and the length of the cable.

2. The variable flow field which occurs in the ocean is not the uniform flow achieved in the laboratory. Since the frequency of the oscillating fluid force which causes strumming is proportional to the velocity of flow past the cable, the variation in relative water velocity from one location on the cable to another results in competing vibration frequencies. For the cable to be locked-in and vibrate in a single mode, a large proportion of the cable would have to be subjected to a dominant steady current. Ocean currents are likely to exhibit both spatial and temporal variations inhibiting modal vibration.

3. Cables in the ocean are attached to buoys, ships, or moors and exhibit catenaries, even in nearly uniform flow. This means that the cable forms a variable angle with the flow. A yawed cylinder has been shown<sup>10</sup> to have a vortex shedding frequency dependent upon the yaw angle  $\alpha$

$$f_s(\alpha) = \frac{StV}{d} \cos \alpha \quad (35)$$

This can, again, give rise to oscillating forces acting at different frequencies upon different sections of the cable.

4. If the forcing function is not acting in concert along the entire cable length, then it becomes pertinent to consider how a particular vibration propagates in the cable to ascertain whether localized strumming can force the whole cable into lock-in. The logarithmic decrement is the natural logarithm of the ratio of the amplitude of one oscillation to that of the next which has the same polarity when no external forces are applied to maintain the oscillation. Then, if  $a_1$  is the amplitude of the vortex-induced vibration,  $a_2$  is the next,  $a_3$  the next, and so on, the log decrement  $\delta$  is:

$$\delta = \ln \frac{a_1}{a_2} = \ln \frac{a_2}{a_3} = \ln \frac{a_{n-1}}{a_n} \quad (36)$$

and

$$e^\delta = \frac{a_1}{a_2} = \frac{a_2}{a_3} = \frac{a_{n-1}}{a_n} \quad (37)$$

then,

$$\frac{a_1}{a_n} = \frac{a_1}{a_2} \cdot \frac{a_2}{a_3} \dots \frac{a_{n-1}}{a_n} = e^{(n-1)\delta} \quad (38)$$

so that

$$\ln \frac{a_1}{a_n} = (n-1)\delta \quad (39)$$

or

$$\delta = \frac{1}{n-1} \ln (a_1/a_n) \quad (40)$$

From vibration theory,

$$\delta = \frac{\pi c}{m \omega_n} \quad (41)$$

where  $c$  is the damping. Using the approximation of eq. (20)

$$\delta = \frac{4.5 \pi^2 \rho \nu}{m \omega_n} \sqrt{\frac{\omega_n d^2}{4 \nu}} \quad (42)$$

where

$$\omega_n = 2 \pi f_n = 2 \pi \frac{StV}{d} \quad (43)$$

therefore,

$$\delta = 19.33 \left( \frac{\rho d^2}{m} \right) / \sqrt{N_{Re}} \quad (44)$$

If it is assumed that the vibration is sufficiently damped when

$$a_1/a_n = 20 \quad (45)$$

then

$$\frac{2.996}{(n-1)} = \frac{19.33}{\sqrt{N_{Re}}} \left( \frac{\rho d^2}{m} \right) \quad (46)$$

and

$$n = 1 + 0.155 \left( \frac{m}{\rho d^2} \right) \sqrt{N_{Re}} \quad (47)$$

That is, the  $n$ th vibration has been damped sufficiently to be considered no longer propagating along the cable. This can be related to distance by the wavelength  $\lambda$ , obtained from the string equation, eq. (5)

$$\lambda = \frac{1}{f_n} \sqrt{\frac{T}{m}} \quad (48)$$

or

$$\lambda = \frac{d}{StV} \sqrt{\frac{T}{m}} = 4.76 \frac{d}{V} \sqrt{\frac{T}{m}} \quad (49)$$

For the MIT cable in experiment 5, for example,  $d = 0.16$  inch,  $T \approx 46$  lbs.,  $m \approx 0.00077$  slugs/ft (including hydrodynamic mass) at  $V = 1.0$  ft/s or  $N_{Re} \approx 1026$ ,

$$n \approx 12 \quad (50)$$

$$\lambda = 15.5 \text{ ft} \quad (51)$$

and

$$n\lambda = 186 \text{ ft} \quad (52)$$

which is small in comparison to the length of cable tested (950 ft).

5. When these factors are taken into account, it is not reasonable to expect a lock-in behavior where the entire cable is strumming in a vibration mode described by the string equation. It is not clear, however, how all these factors interact in producing a composite drag on the cable, and further investigation under more controlled conditions is required.

## RESULTS

1. Employing independent methods of measurement, coefficients of drag for long cables were found to be in the 1.0 to 2.0 range, averaging approximately 1.4 in the Reynolds number range of 500 to 2000.
2. No correlation was found between the vibrations measured at one location on the cable and those measured simultaneously at another location, where separation distances were as small as 100 feet.

## CONCLUSIONS

1. The coefficient of drag for long cables in realistic flow is less than the coefficient of drag obtained for short cables in uniform flow.
2. Sustained modal vibration, or lock-in, does not occur in long cables with catenaries and/or in non-uniform flow.
3. The top angle tilt-tension measurement method and the accelerometer method are both useful in the analysis of cable drag and yield compatible results.
4. Further testing is required to extend the drag coefficient measurements over a larger Reynolds number range and to evaluate further the behavior of long cables as it relates to short cable behavior under laboratory conditions.

## RECOMMENDATIONS

1. A drag coefficient of 1.4 should be used for long cables in the Reynolds number range of 500 to 2,000, and an increased  $C_D$  following the curve shown in Figure 15 should be used for larger Reynolds numbers.
2. Further testing should be conducted to measure drag and vibration correlation in cables of various lengths, diameters, and densities ( $m/\rho d^2$ ) over a range of velocities to establish  $C_D$  vs. Reynolds number as affected by cable length-to-diameter and cable stiffness.

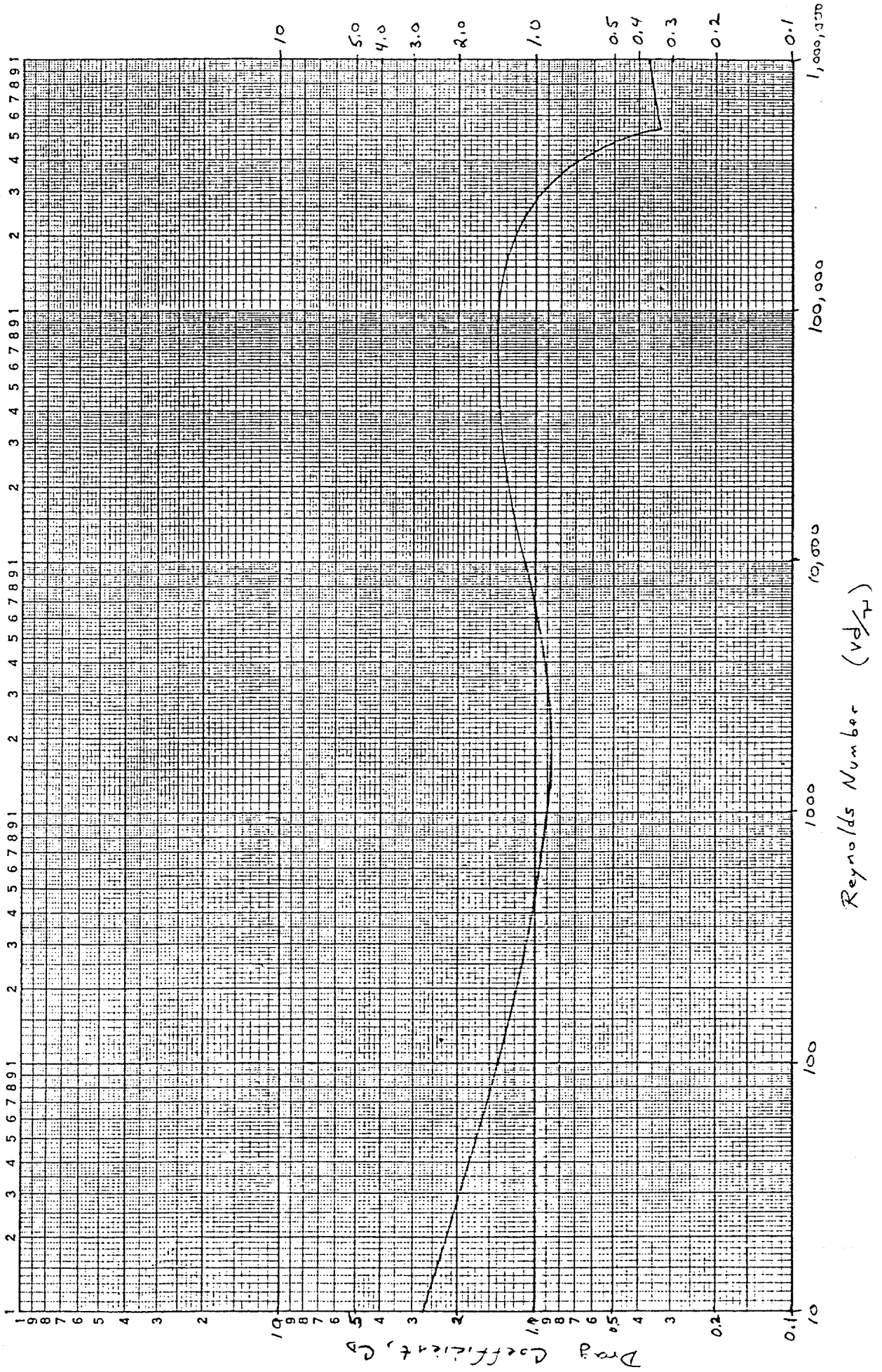
## REFERENCES

1. Dale, J.R., Menzel, H., and Mc Candless, J., "Dynamic Characteristics of Underwater Cables - Flow Induced Transverse Vibrations", NAVAIRDEVCON Report NADC-AE-6620, Sep 1966
2. Dale, J.R., and Holler, R.A., "Vortex Wakes from Flexible Circular Cylinders at Low Reynolds Numbers", NAVAIRDEVCON Report NADC-AE-7011, July 1970
3. Dale, J.R., and Holler, R.A., "Spurious Signals from Cable-Suspended Sonar Systems", J. of Hydronautics Vol 3, No. 2, April 1969
4. Dale, J.R., Mc Candless, J.M., and Holler, R.A., "Water Drag Effects of Flow Induced Cable Vibrations", ASME Paper 68-WA/FE-47, Dec 1968
5. Vandiver, J.K., and Griffin, O.M., "Measurements of the Vortex Excited Strumming Vibrations of Marine Cables", Ocean Structural Dynamics Symposium '82 Proceedings, Oregon State University, Sep 1982
6. Mc Glothlin, J.C., "Drag Coefficients of Long Flexible Cylinders Subject to Vortex Induced Oscillations", Masters Thesis, Massachusetts Institute of Technology, Department of Ocean Engineering, 1982
7. Alexander, C.M., "The Complex Vibrations and Implied Drag of a Long Oceanographic Wire in Cross-Flow", Ocean Engineering Vol. 8, 1981
8. Skop, R.A., Griffin, O.M., and Ramberg, S.E., "Seacon II Strumming Predictions", NRL Memorandum Rpt 3383, Oct 1976
9. Griffin, O.M., Ramberg, S.E., Skop, R.A., Meggitt, D.J., and Sergev, S.S., "The Strumming Vibrations of Marine Cables: State of the Art", Civil Engineering Laboratory Technical Note N-1608, May 1981
10. Chiu, W.S., and Lienhard, J.H., "On Real Fluid Flow Over Yawed Circular Cylinders", ASME Paper No. 67-WA/FE-11, Aug 1967

## ACKNOWLEDGEMENT

This paper is the result of the teamwork of a number of participants in the planning and execution of the test and the analysis of its results. Dr. J. Kim Vandiver and Mr. Yang-Hann Kim of MIT were responsible for a major portion of this test and will be reporting their detailed results in a separate paper. Mr. John Brett of NADC was invaluable in his role as engineer in charge of instrumentation, and without his meticulous attention to detail much valuable data might have been lost. Mr. Jim Hannon and Mr. Mike Sawchuk of Sippican Corporation provided their time and expertise to reduce on-site current data. Mr. Frank Marshall of NADC and Mr. Peter Van Hamm of Sanders Associates, Inc., as well as all of the aforementioned participants, made a significant contribution to the day to day conduct of this test. A special thanks is accorded to Mr. Clifford Ives, master of the YFN-1126; Mr. Robert Tyger, engineer; and the crew of the YFN-1126 and R/V SAXTON for their enthusiastic help in conducting the test and their willingness to attempt some of the out-of-the-ordinary maneuvers that made this test successful.

Figure 1 Drag Coefficient vs Reynolds Number for an Infinite Cylinder



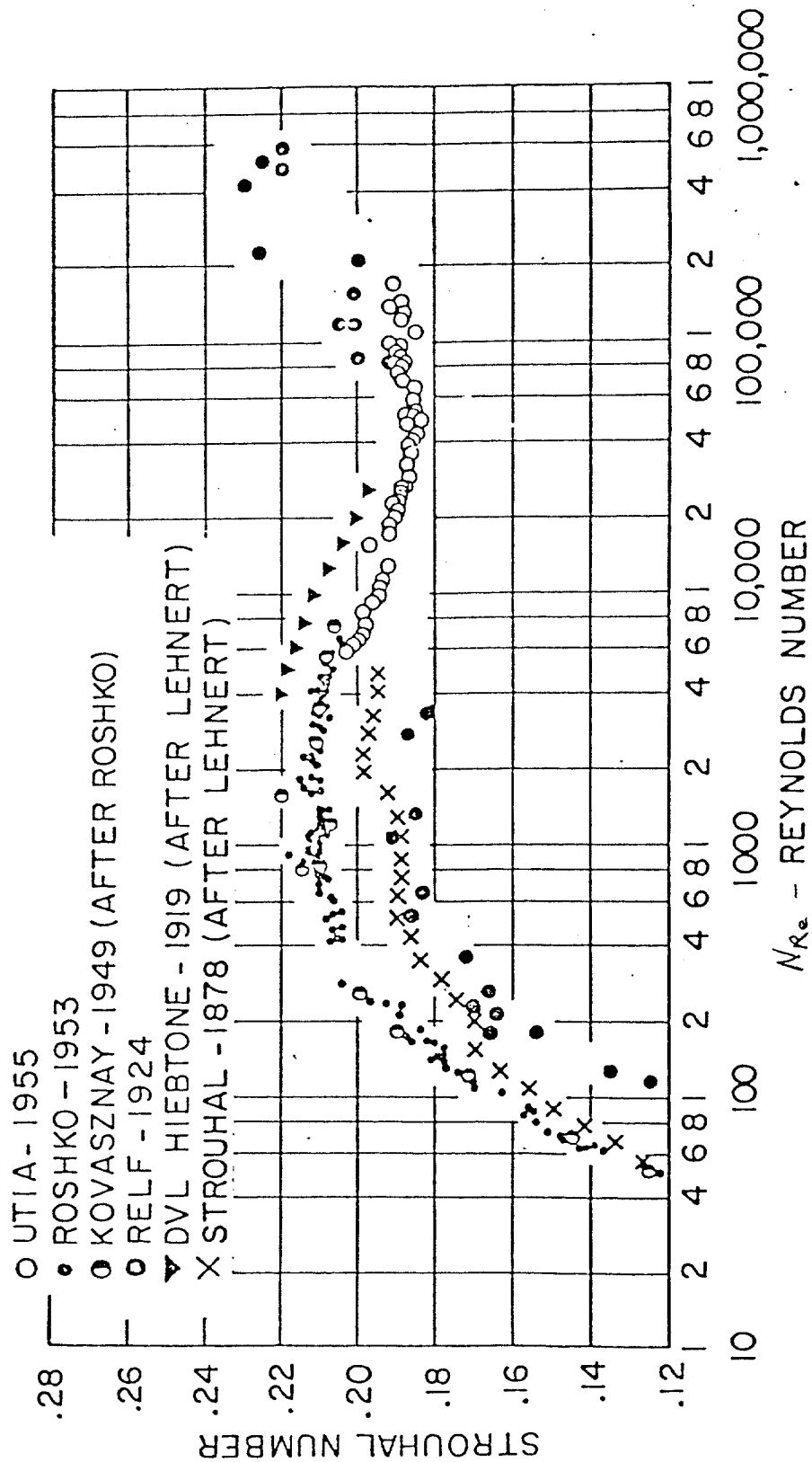
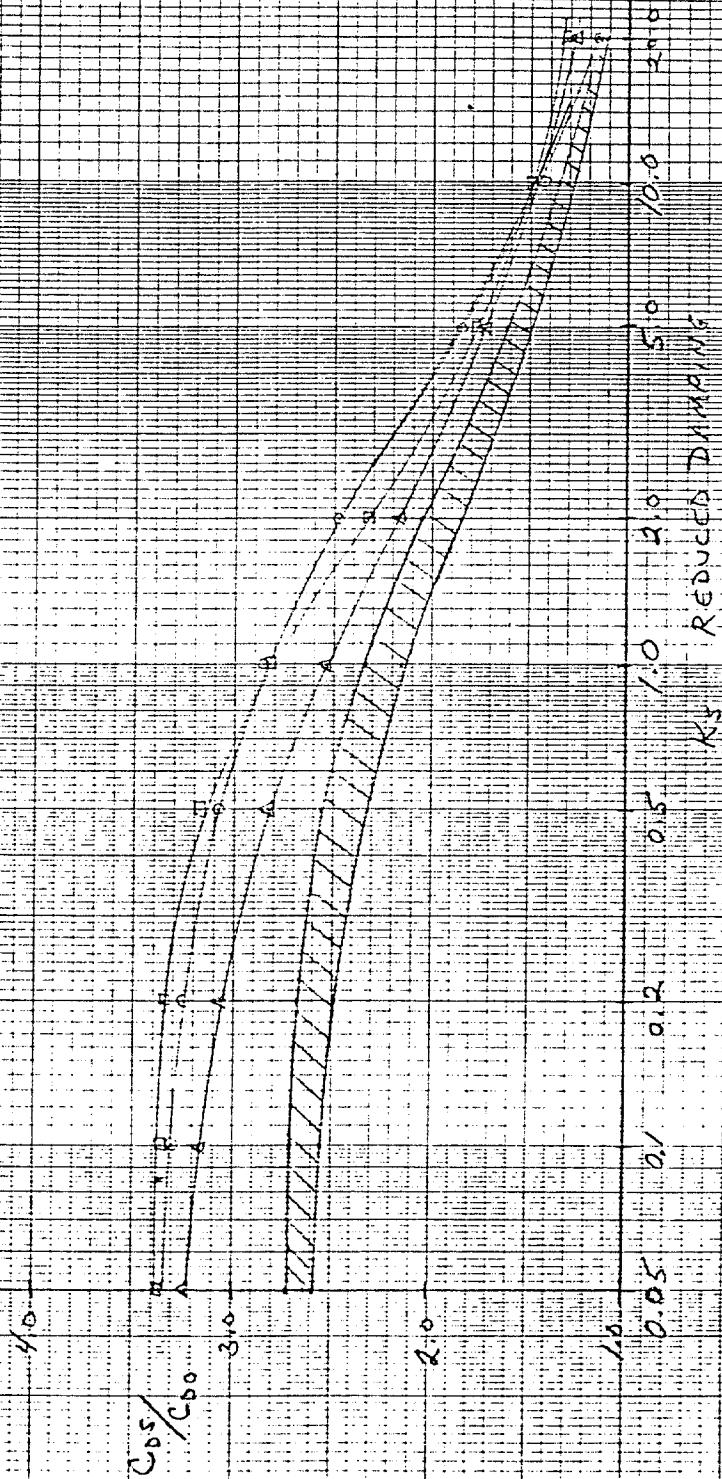


Figure 2: Variation of  $St$  versus  $Re$  for rigid stationary cylinders



Figure 3: Ratio of Streaming Drag Coefficient to Non-Streaming Drag Coefficient at the Antinode as a Function of Reduced Damping.

O GRIFIN, STUR, KRAMBERG } ANTINODE DRAG FOR  
 A BLEVINS } SINUSOIDAL MODE  
 □ SARPAYA } SHAPE  
/// McCLATHLIN or } AVERAGE DRAG FOR  
 VANDIVER & GRIFFIN } FLEXIBLE  
 CYLINDERS  
 IN MODAL  
 VIBRATION



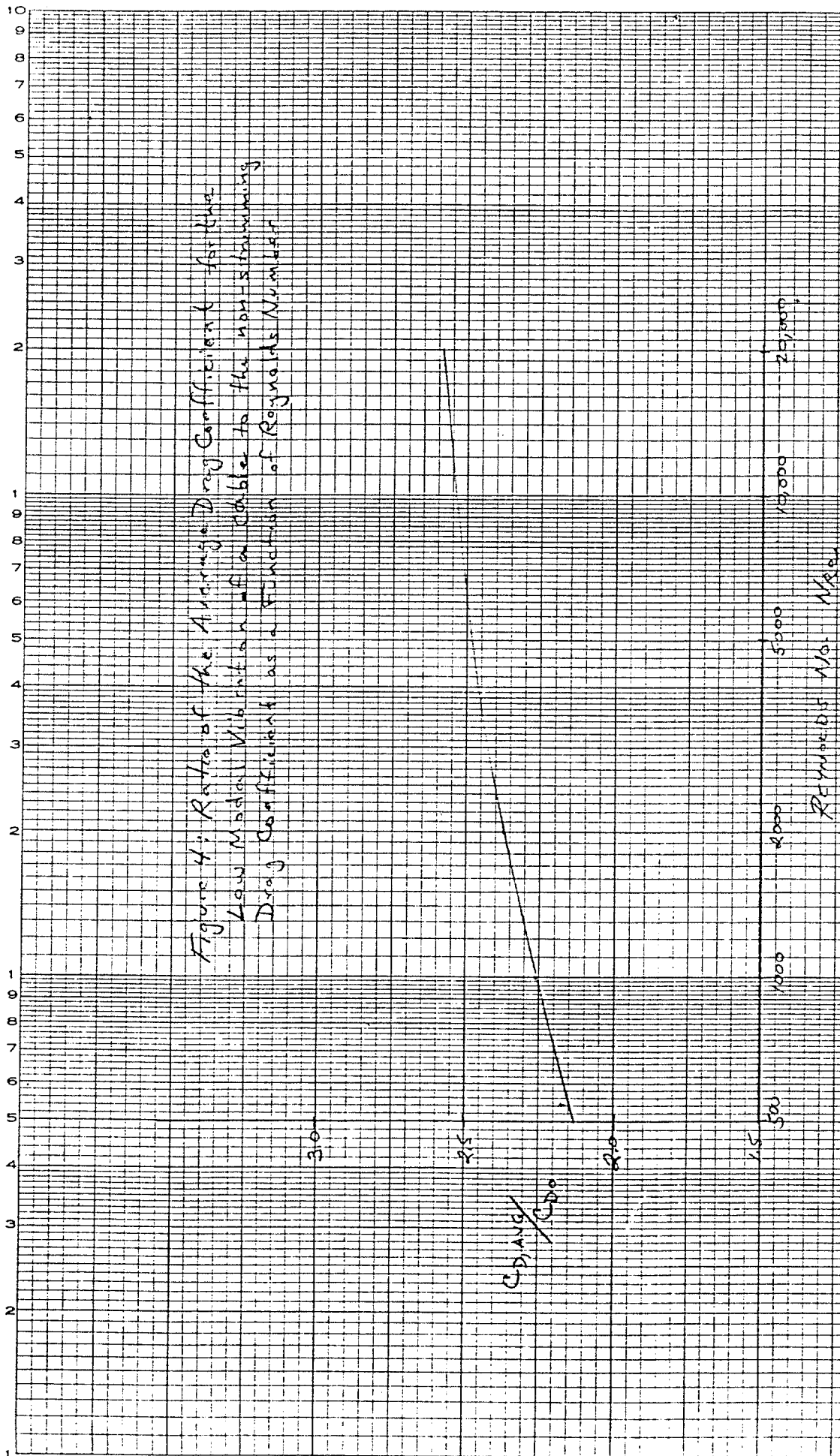


Figure 5: The Average Drag Coefficient of a Low Model  
Streamline Airfoil as a Function of Reynolds Number

3.0

$C_D$  Avg

2.0

1.0

500

1000

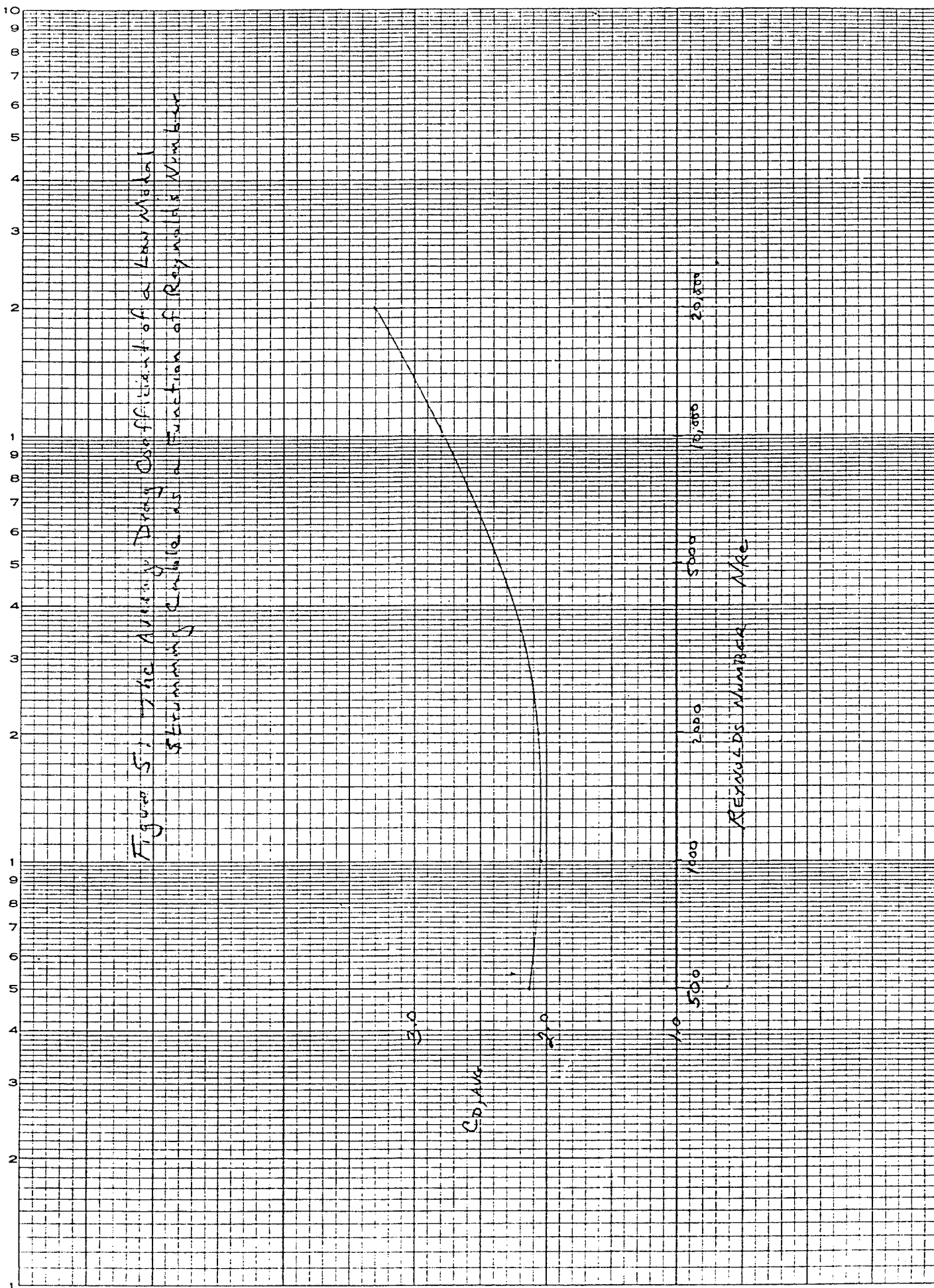
2500

5000

10,000

20,000

REYNOLDS NUMBER  $N_{Re}$



$$C_D A = 0.32$$

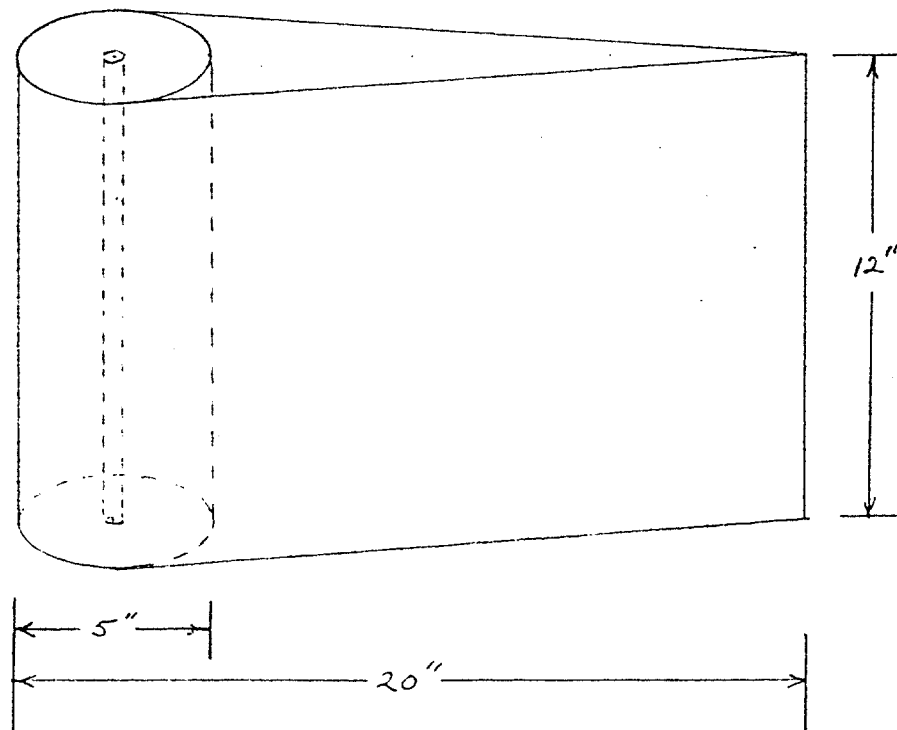
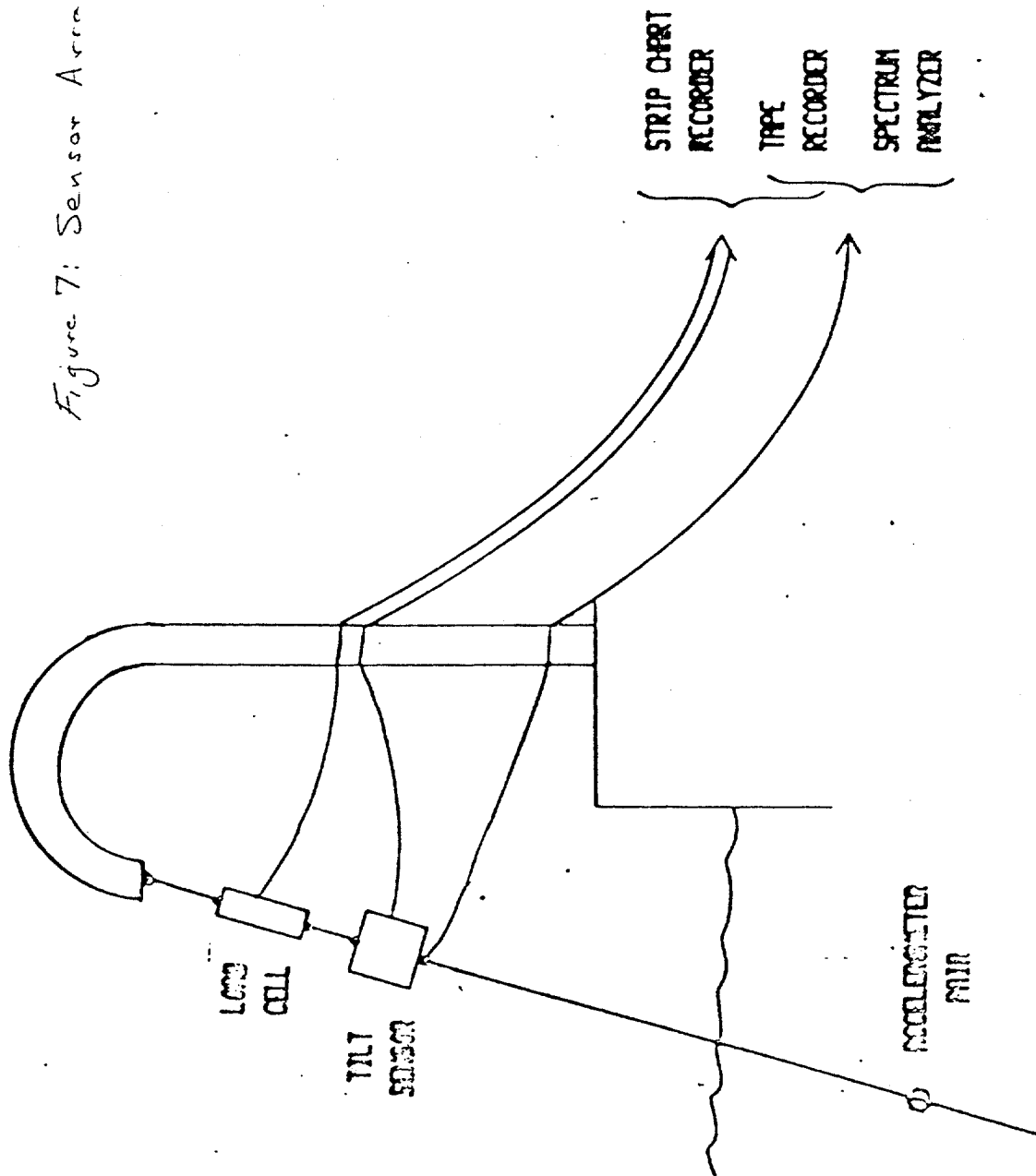


Figure 6: Faired Cylinder Lower Unit

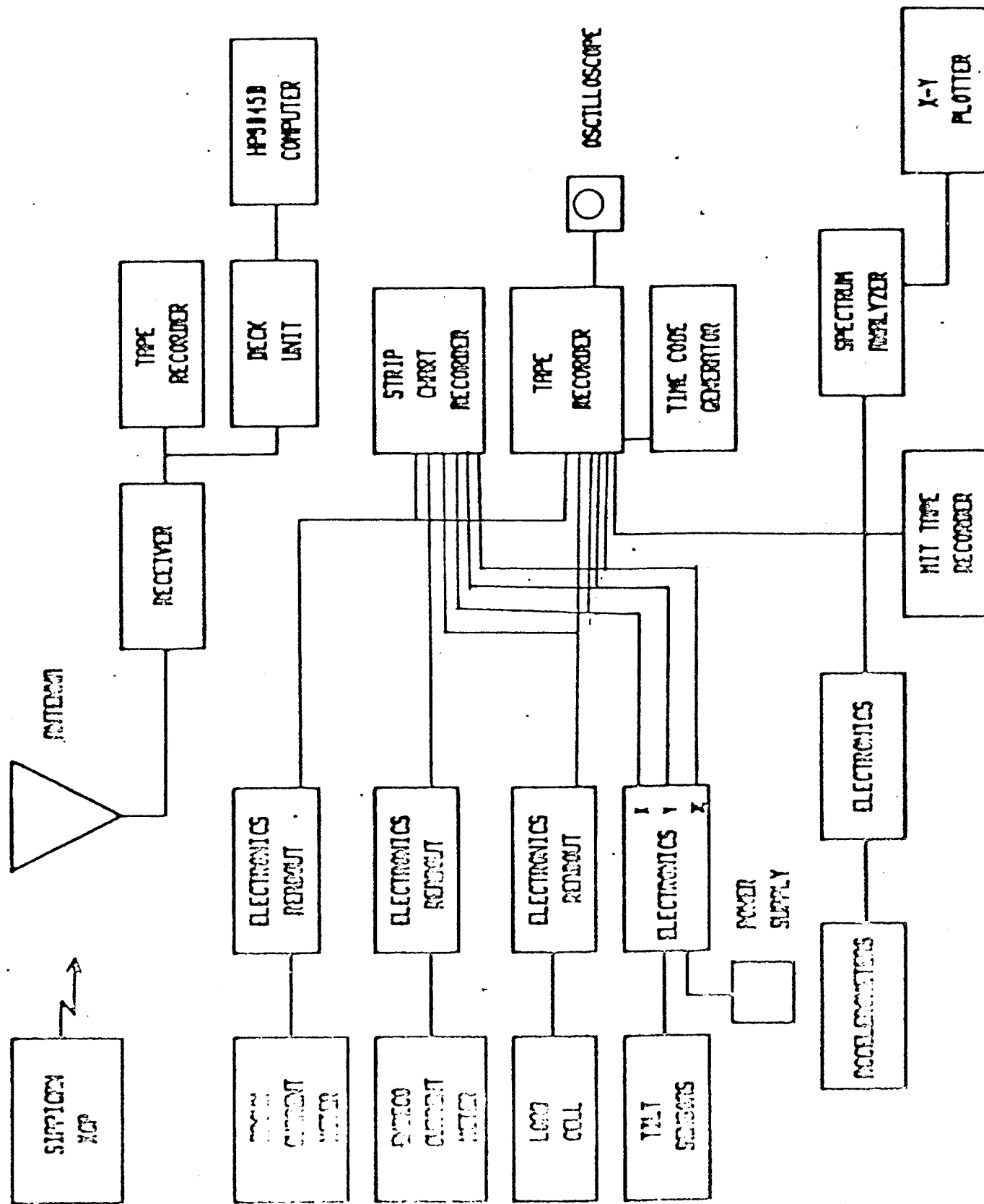
Figure 7: Sensor Arrangement

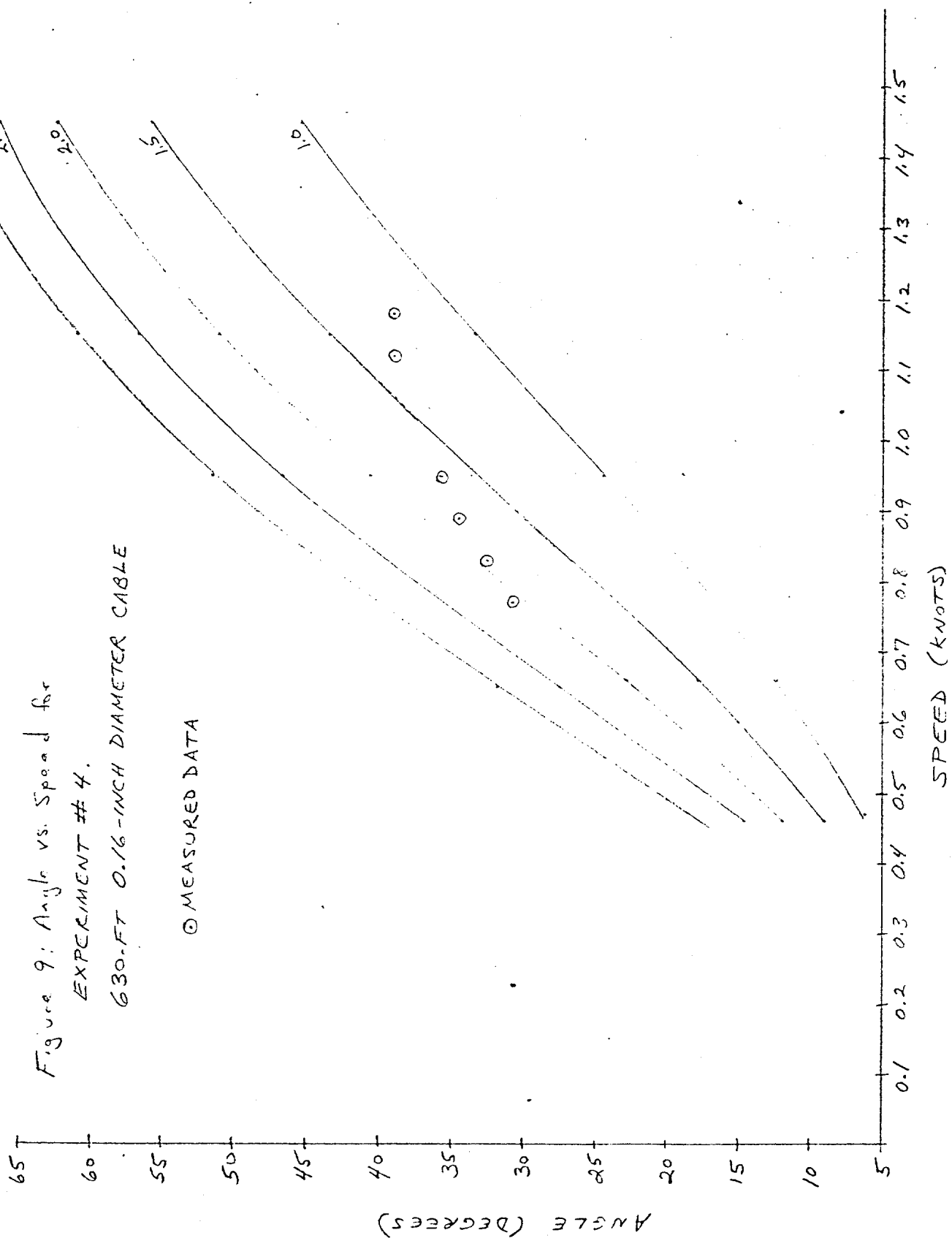


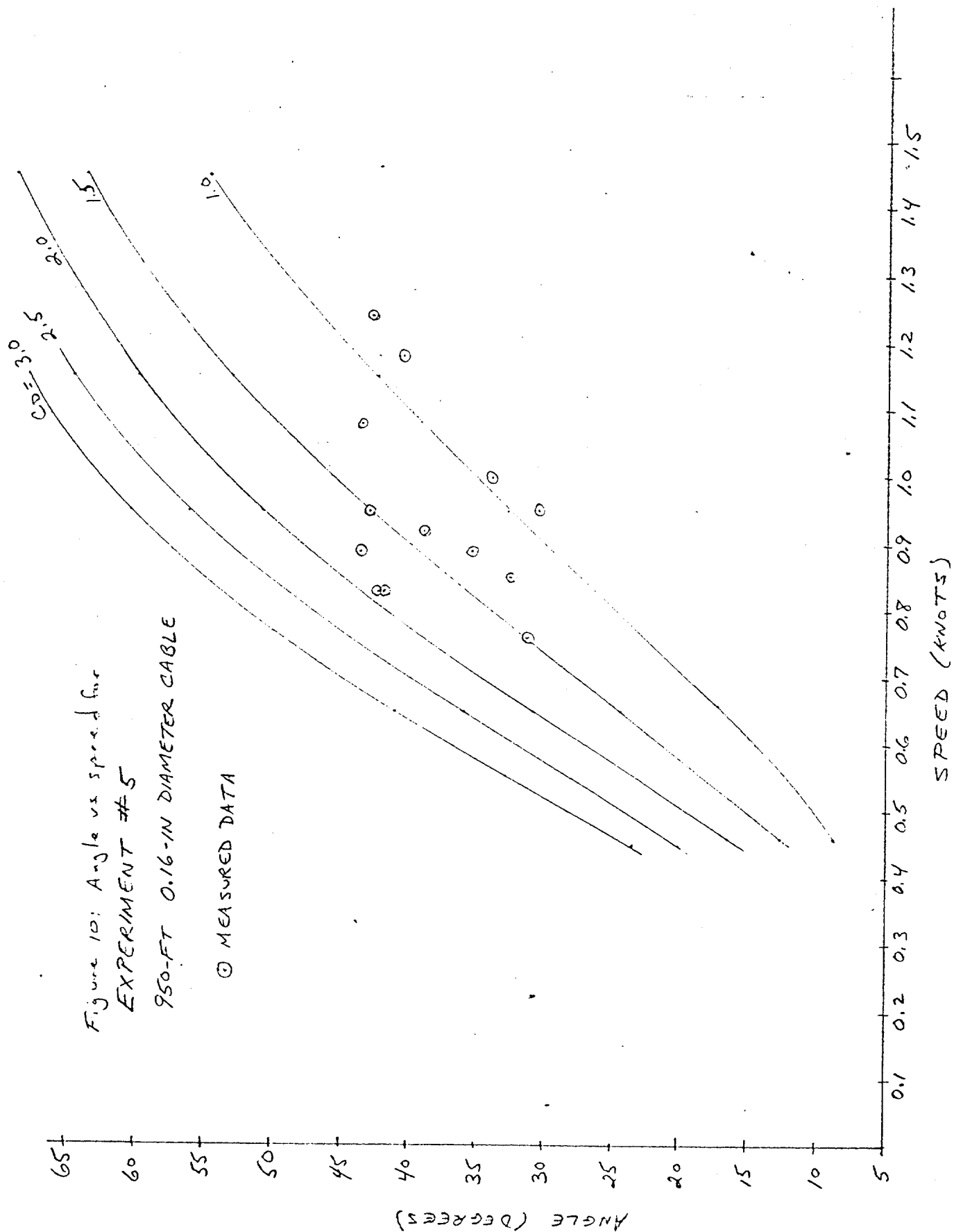
**FACILITY USED:**

- NREC DEEP WATER FACILITY, ST. CROIX
- STABLE PLATFORM (137' X 34' DARGE) ON 10,000 FT MOORING
- 500 MILES OFFSHORE

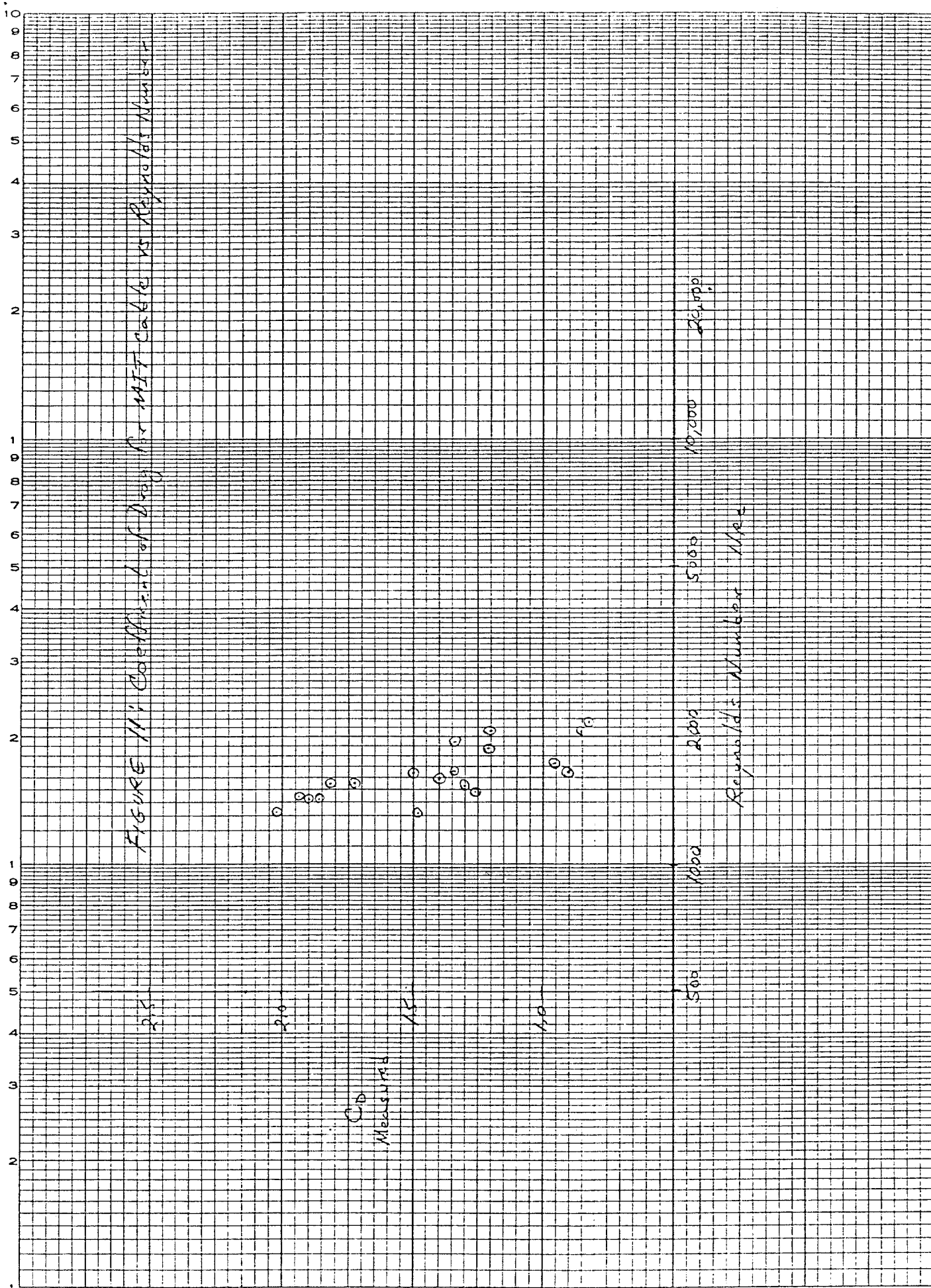
Figure 8: The Experimental SET-UP

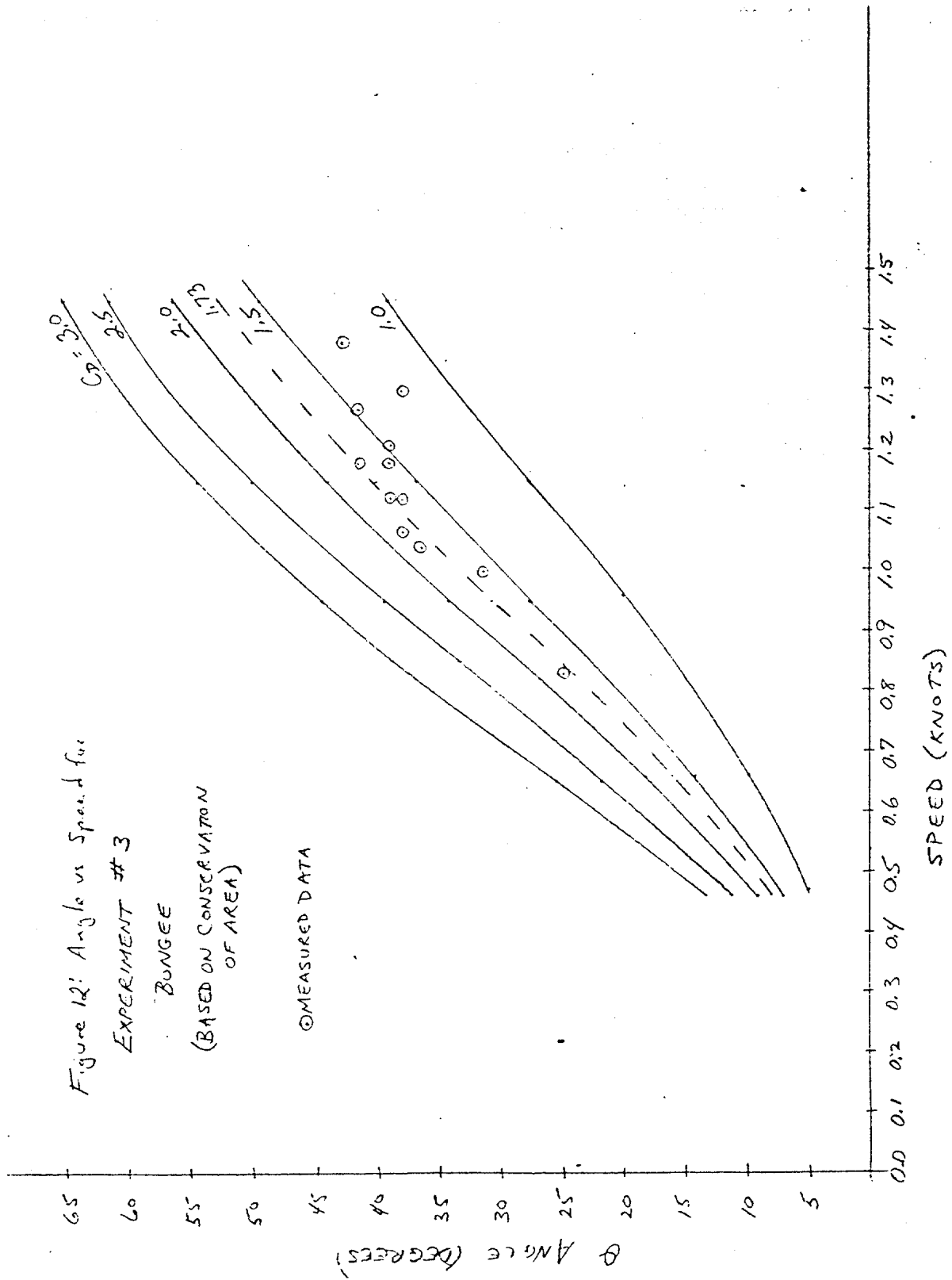












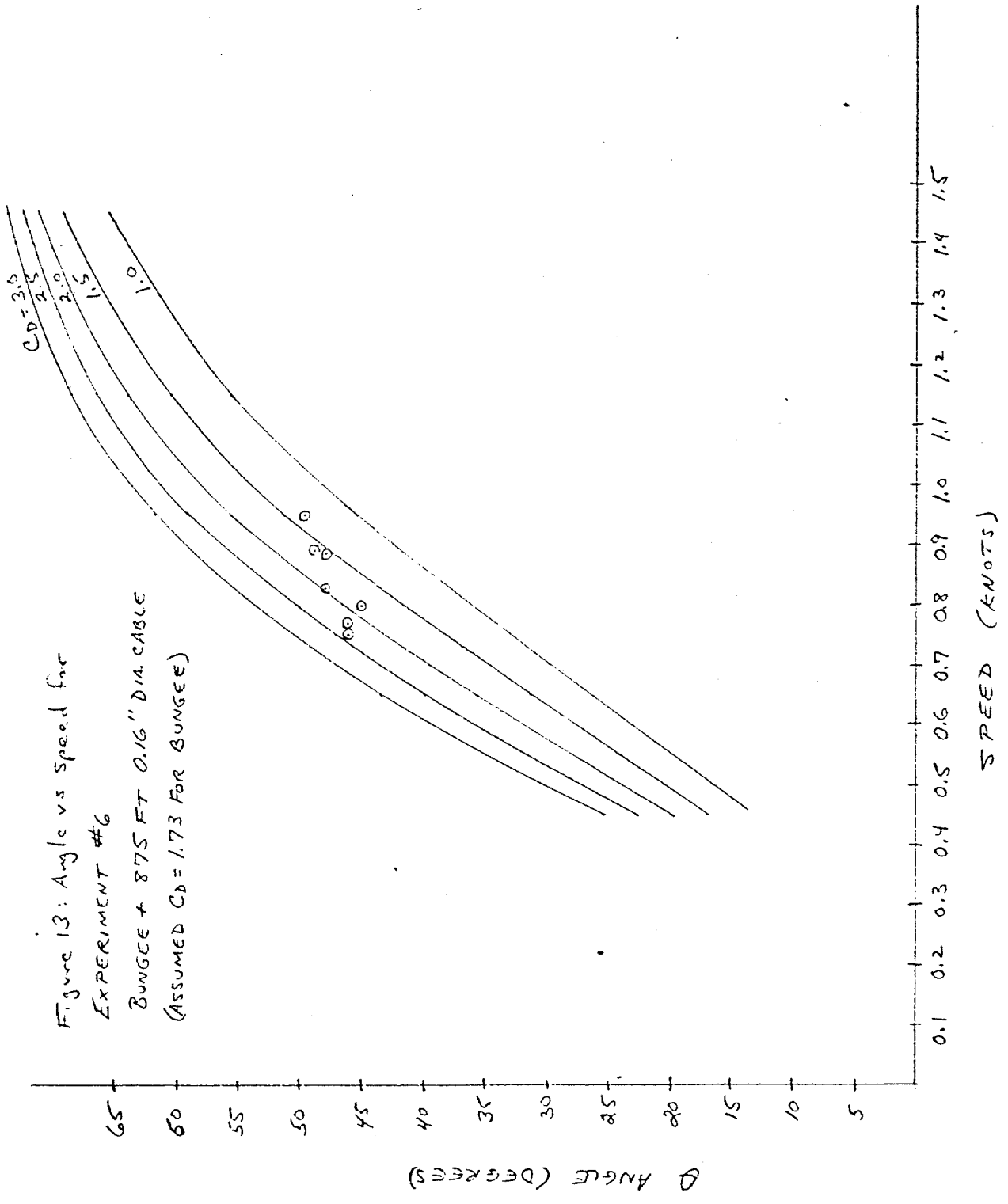
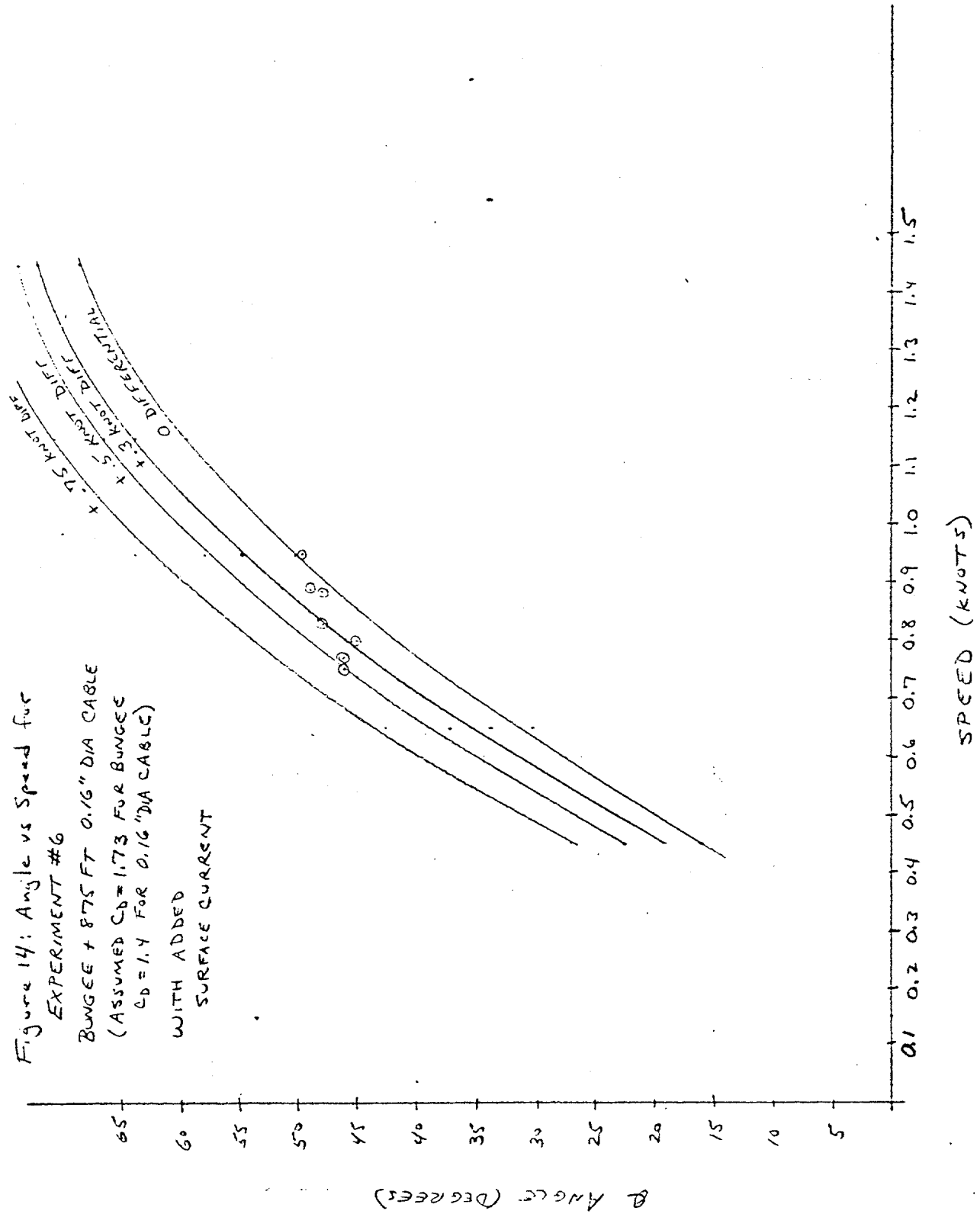
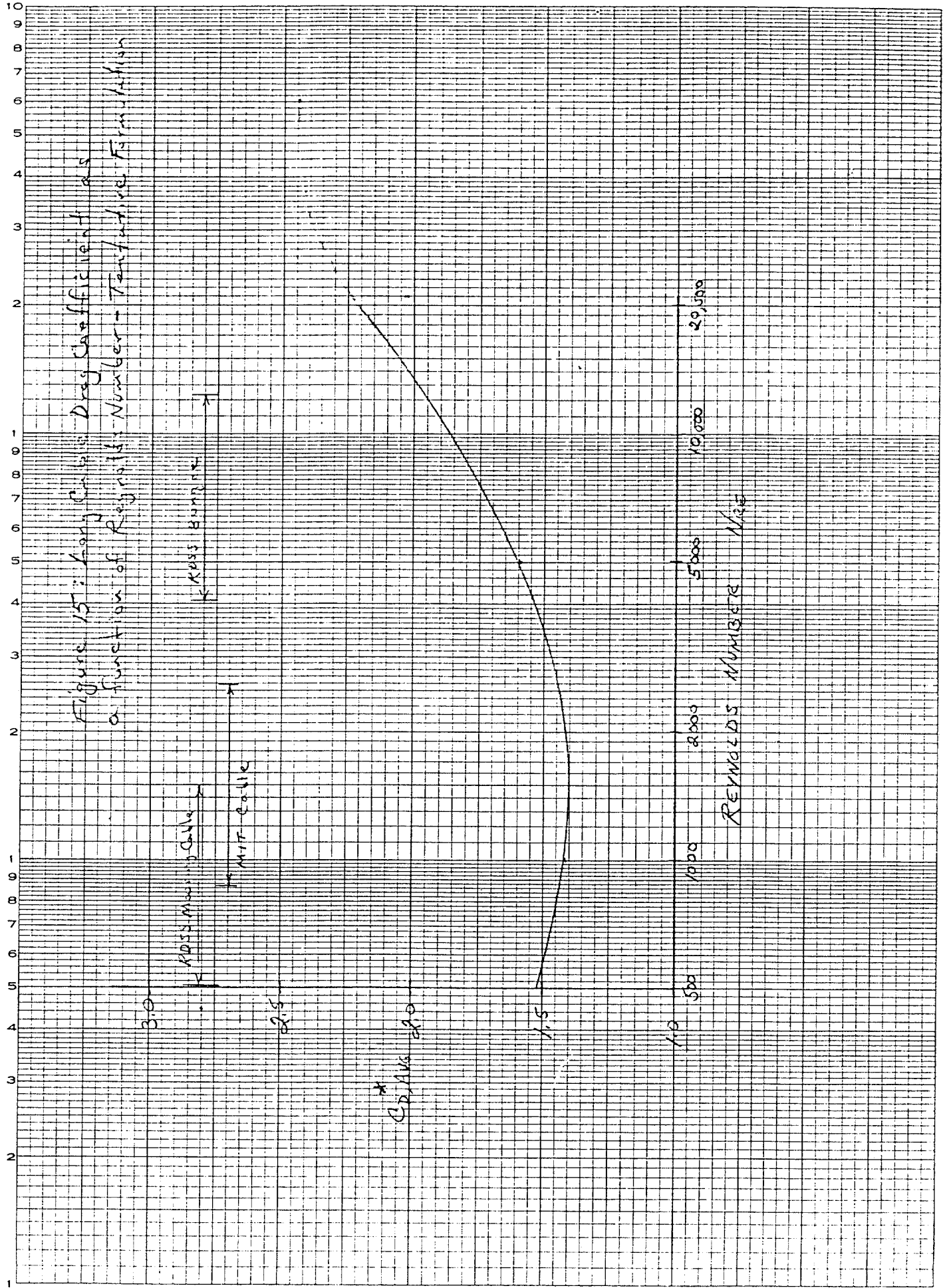
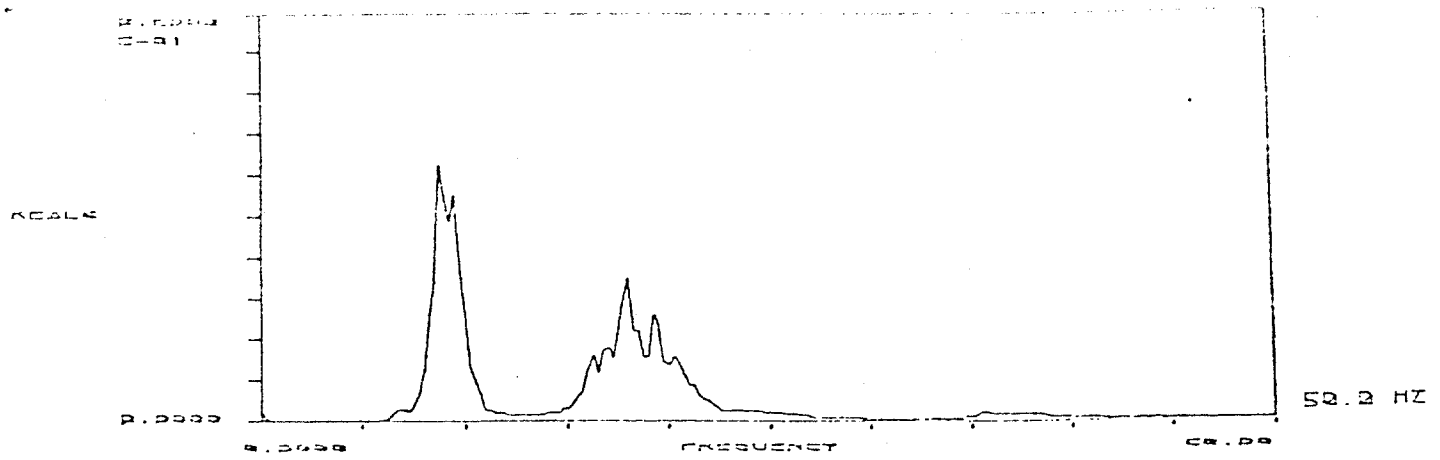


Figure 14: Angle vs Speed for  
EXPERIMENT #6  
BUNGEE + 875 FT 0.16" DIA CABLE  
(ASSUMED  $C_D = 1.73$  FOR BUNGEE  
 $C_D = 1.4$  FOR 0.16" DIA CABLE)

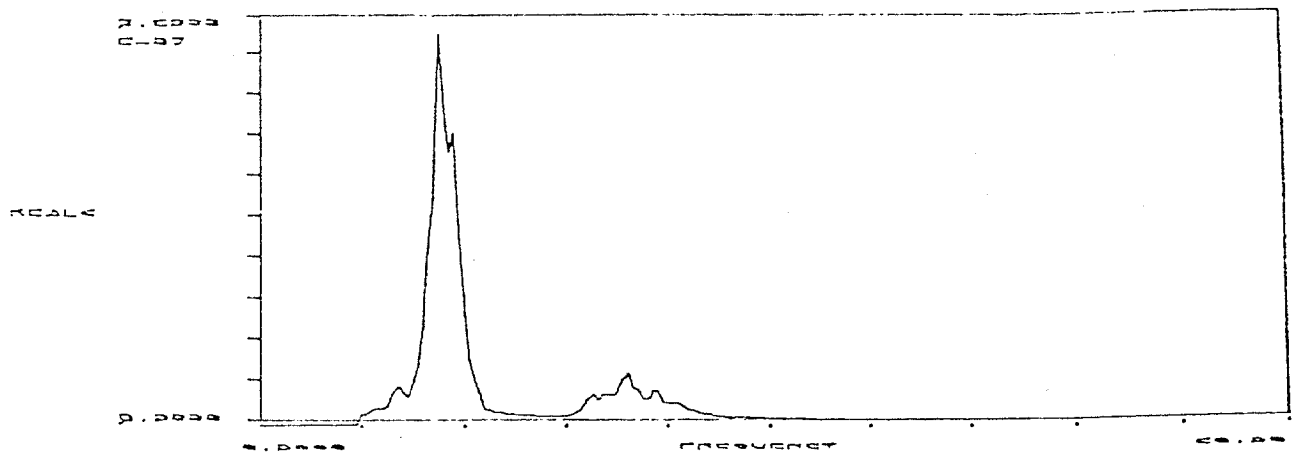
WITH ADDED  
SURFACE CURRENT



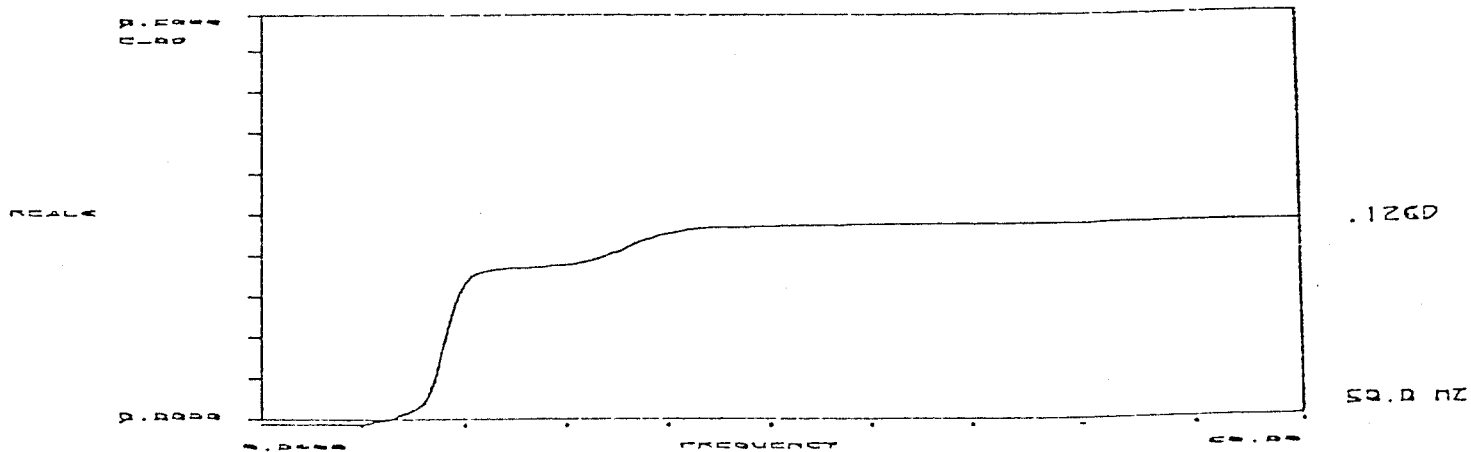




ACCELERATION SPECTRUM



DISPLACEMENT SPECTRUM

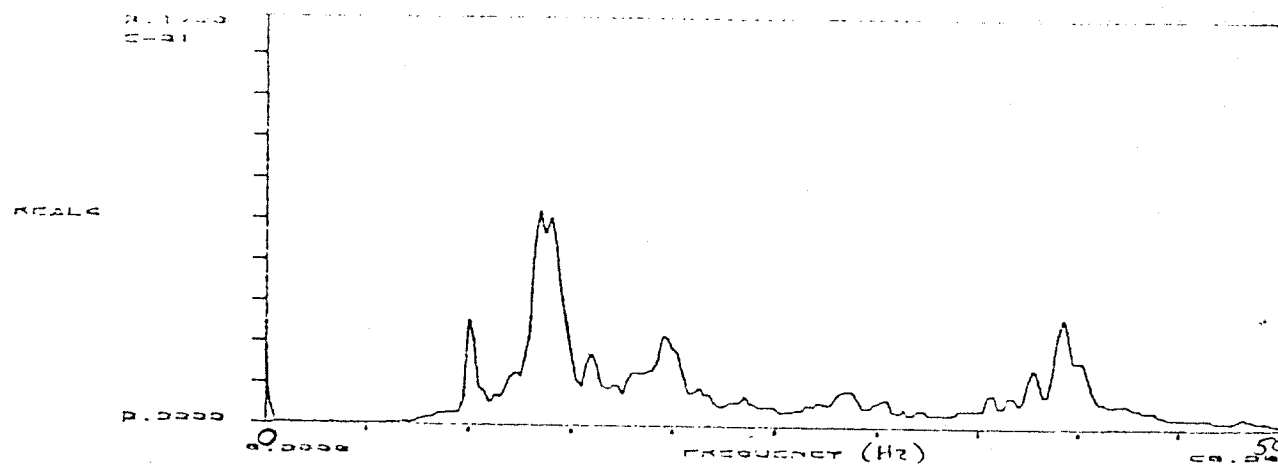


RMS DISPLACEMENT

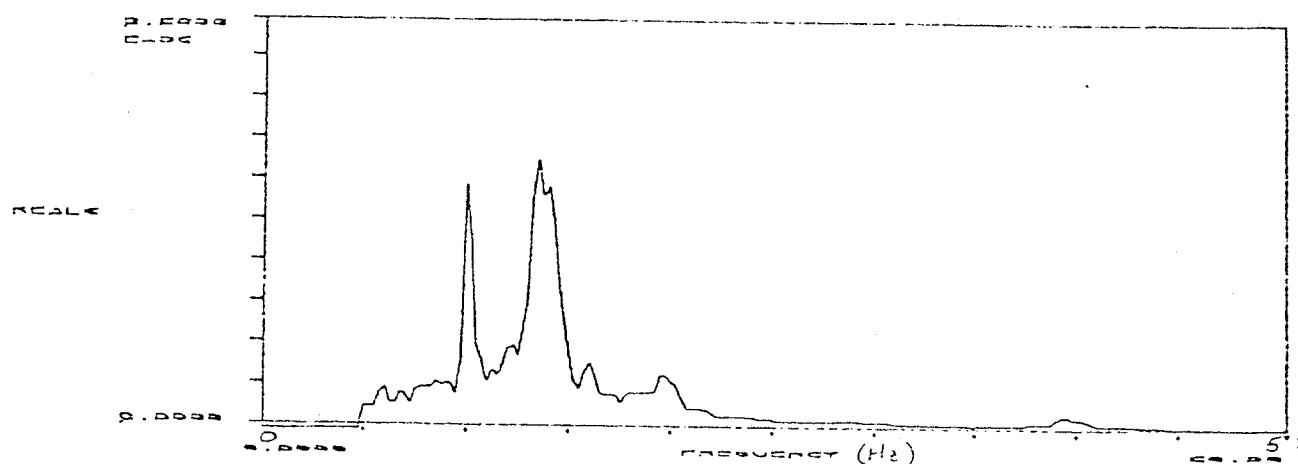
DOUBLE INTEGRATION OF ACCELERATION

ST. CROIX, ST. 1, ACCEL #5, L-950 FOOT

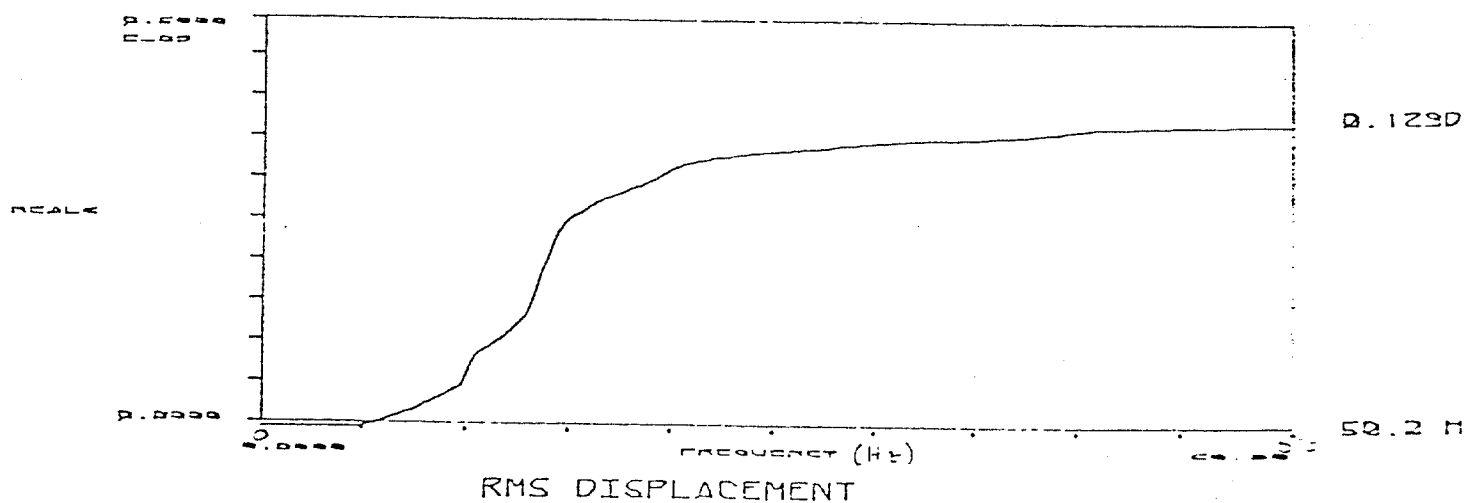
Figure 17: Acceleration Data from Experiment #1 350 ft Deep



ACCELERATION SPECTRUM



DISPLACEMENT SPECTRUM



DOUBLE INTEGRATION OF ACCELERATION

ST. CROIX, ST. 1, ACCEL #3, L-950 FOOT

Figure 16: Accelerometer Data from Experiment #1, 75 ft Down the C